Pergamon

0013-7944(95)00151-4

Engineering Fracture Mechanics Vol. 53, No. 6, pp. 917–928, 1996

0013-7944/96 $15.00 + 0.00

A CONTINUUM DAMAGE MECHANICS MODEL FOR VOID GROWTH AND MICRO CRACK INITIATION

S. DHAR, RAJU SETHURAMAN† and P. M. DIXIT

Department of Mechanical Engineering, Indian Institute of Technology, Kanpur 208016, India

Abstract—A damage mechanics model is proposed to study the void growth and crack initiation. J_2 incremental flow theory along with a damage variable is used to model the material behaviour in elasto-plastic regime. Large deformation (large rotation and finite strain) finite element analysis is carried out for five different cases. In all the cases it is observed that the triaxiality and the plastic strain play an important role in void growth and crack initiation in ductile material. A failure curve is obtained for the material AISI-1090 spheroidised steel. Finally, it is concluded that the critical value of the damage variable can be taken as a crack initiation parameter.

NOTATION

a	void dimension (Fig. 1)
a_1	coefficient of damage growth law
a_2	coefficient of damage growth law
$\mathbf{a}$	flow vector
A	area of cross-section at the necked region
A_0	area of cross-section of the unit cell (Fig. 1)
A_n	area of cross-section of the unit cell between the voids (Fig. 1)
$\bar{A}_n$	effective area void fraction
b	void dimension (Fig. 1)
c	coefficient of damage growth law
$[C]$	elastic constitutive matrix
$[C^{EP}]$	elasto-plastic constitutive matrix
d	intervoid spacing (Fig. 1)
$\mathbf{d}\epsilon$	incremental strain in vector form
$\mathbf{d}\sigma$	incremental stress in vector form
d_0	initial diameter of cylindrical specimen
d_c	current diameter of cylindrical specimen
D	damage variable
D_c	critical value of damage variable
E	Young's modulus
F	plastic potential
F_1	plastic potential associated with yielding
F_D	plastic potential associated with damage
H	hardening parameter
K	hardening parameter
n	hardening parameter
P	load
r	internal hardening variable
R	virtual work done by surface tractions
R^*	effective hardening stress variable
S_{ij}	2nd Piola Kirchoff stress tensor
$-Y$	elastic damage energy release rate
ΔA	infinitesimal area
ΔA_v	area of void traces contained in ΔA
Δu_i	incremental displacement vector
Δe_{ij}	linear part of incremental strain tensor
$\Delta \eta_{ij}$	non-linear part of the incremental strain tensor
ϵ_{ij}	Green–Lagrange strain tensor
$\dot{\epsilon}_{ij}$	strain rate tensor
$\dot{\epsilon}^p_{ij}$	plastic part of strain rate tensor
ϵ_{eq}	equivalent strain
ϵ^p_{eq}	equivalent plastic strain
$\dot{\epsilon}_{eq}$	equivalent strain rate
$\dot{\epsilon}^p_{eq}$	equivalent plastic strain rate

†Corresponding author.

λ scalar in a damage evolution law
ν Poisson's ratio
σ_0 initial yield stress in uniaxial tension
σ_1 maximum principal stress
σ_n plastic constraint stress
σ_m^* mean part of effective stress tensor
σ_{eq} equivalent stress
σ_{eq}^* effective equivalent stress
σ_{ij} Cauchy stress tensor
σ_{ij}^* effective stress tensor
σ_{ij}' deviatoric part of Cauchy's stress tensor
$\sigma_{ij}^{*\prime}$ deviatoric part of effective stress tensor
$\mathring{\sigma}_{ij}$ Jaumann stress rate
$\frac{\sigma_m}{\sigma_{eq}}$ triaxiality
Ω_{ij} spin tensor.

1. INTRODUCTION

SATISFACTORY IDENTIFICATION of fracture criteria for ductile material has not been available in the literature till today. It has been observed from metallurgical test results that ductile fracture occurs mainly due to void nucleation, growth and finally coalescence into a crack. Earlier models of McClintock [1] and Rice and Tracey [2] considered single void in a continuum. These models assumed a pre-existed finite size void in a continuum and hence did not consider any void nucleation phenomena. Based on Berg's [3] theory of dilatational plasticity, Gurson [4] proposed a plastic potential taking into account both the void nucleation and growth. Many research workers used the Gurson model taking a critical void volume fraction equal to 1.0 for micro crack initiation; but, from the experimental test [5], it was observed that at the final stage of void growth, the void coalesces by internal necking. This phenomenon starts at a critical void volume fraction which is well below 1.0 and then increases rapidly to 1.0.

Recently, based on continuum thermodynamics, Lemaitre [6] proposed a damage model for elasto-plastic case. The concept of "effective" stress and strain equivalence is used in deriving this model. He performed an experiment to find the critical value of the damage variable from the change of elastic modulus in the one dimensional tensile test. However, his damage evolution law did not account for void nucleation. On the other hand, the experiment of Le Roy *et al.* [7] which measures the growth of area void fraction with one dimensional strain seems to give a more consistent damage evolution law, as the damage is identified as the area void fraction in a particular plane.

All the models cited above require a critical value of a material parameter for micro crack initiation which has to be determined either by experiment or by appropriate micro model based on void coalescence. In all the studies done by earlier investigators, either the effect of void nucleation and growth was not considered simultaneously, or the micro crack initiation criterion was not based on void coalescence. Moreover, the void nucleation and the growth ahead of the crack tip need stress analysis which has to take into account the effect of finite strain and large rotation.

The objectives of this paper are to define a damage variable properly, to establish its critical value as a material property and to extend it as a parameter for micro crack initiation. Lemaitre's [6] Continuum Damage Mechanics model together with experimental results of Le Roy *et al.* [7] are used to derive a damage growth law for ductile materials. Modified Thomason's model [8–10] is used to obtain a criterion for micro crack initiation. Non-linear finite element studies have been done for five different cases of varied geometries to obtain critical values of strain, triaxiality and damage variable for each case.

2. FORMULATION

2.1. *Material characterisation*

Damage represents surface discontinuities in the form of microcracks, or volume discontinuities in the form of microvoids. The description of material behaviour of a damaged

material involves an additional internal variable, called the damage variable, which quantifies the intensity of damage. If it is assumed that cracks and voids are scattered in an isotropic way, then this variable can be represented by a scalar quantity, which in the literature is normally denoted by D. D has been defined in various ways such as change in global mechanical properties (Young's modulus, yield strength, etc.) or change in global physical properties (density, resistance, etc.) or microscopic properties like void volume fraction. Here, the damage variable D is identified as area void fraction at a point, i.e.

$$D = \Delta A_v / \Delta A \tag{1}$$

where ΔA is an "infinitesimal" area around the point in some plane and ΔA_v is the area of the void traces in the plane contained in ΔA. Here, D is considered as a scalar isotropic field quantity, i.e. independent of the plane on which it is defined. The introduction of damage variable leads to the concept of effective stress, i.e. the stress calculated over the effective area $(\Delta A - \Delta A_v)$ that actually resists the forces. Thus, the effective stress tensor σ_{ij}^* at a point is defined as

$$\sigma_{ij}^* = \sigma_{ij}/(1 - D). \tag{2}$$

The conjugate variable corresponding to D is the rate at which the elastic energy is released during damage growth at constant stress. For an isotropic material, the elastic damage energy release rate $(-Y)$ is given by [6]

$$-Y = \frac{\sigma_{eq}^{*2}}{2E} f(\sigma_m^*/\sigma_{eq}^*) \tag{3}$$

where

$$f(\sigma_m^*/\sigma_{eq}^*) = 2(1 + \nu)/3 + 3(1 - 2\nu)(\sigma_m^*/\sigma_{eq}^*)^2. \tag{4}$$

Here, E is the Young's modulus, ν is the Poisson's ratio, σ_m^* is the mean (or hydrostatic) part of the stress tensor σ_{ij}^* and σ_{eq}^* is the equivalent stress related to the deviatoric part $\sigma_{ij}^{*\prime}$ by the relation

$$\sigma_{eq}^* = (\tfrac{3}{2}\sigma_{ij}^{*\prime}\sigma_{ij}^{*\prime})^{1/2}. \tag{5}$$

The constitutive equation for plastic behaviour of a damaged material can be derived from the appropriate plastic potential F. For convenience, F can be decomposed as

$$F = F_1(\sigma_{ij}^*, R^*) + F_D(-Y; r, D). \tag{6}$$

Here, F_D is the plastic potential associated with the damage such that it reduces to zero whenever $D = 0$ and R^* is the effective hardening stress variable which is conjugate to the internal hardening variable r defined by

$$r = (1 - D)\epsilon_{eq}^p \tag{7}$$

$$\epsilon_{eq}^p = \int_0^t \dot{\epsilon}_{eq}^p \, dt \tag{8}$$

$$\dot{\epsilon}_{eq}^p = (\tfrac{2}{3}\dot{\epsilon}_{ij}^p\dot{\epsilon}_{ij}^p)^{1/2}. \tag{9}$$

Here, $\dot{\epsilon}_{ij}^p$ is the plastic part of the strain rate tensor $\dot{\epsilon}_{ij}$. For a material yielding according to von Mises criterion, the first part of the potential F is given by

$$F_1 = (\sigma_{eq}^* - R^*) - \sigma_0 \tag{10}$$

where σ_0 is the yield stress in uniaxial tension. When $D = 0$, σ_{eq}^* and R^* reduce, respectively, to σ_{eq} (equivalent stress corresponding to σ_{ij}) and R (hardening stress variable of an undamaged material), and thus, F_1 reduces to the usual form.

If the form of F_D is known, the evolution of damage can be found from the relation

$$\dot{D} = \lambda \frac{\partial F_D}{\partial(-Y)} \tag{11}$$

where λ is a scalar. However, unlike F_1 the form of F_D is not well established. As a result, experimental observations are used to postulate an appropriate damage evolution law. Based on the model of Lemaitre [6] and the experimental results of Le Roy *et al.* [7], the following law is proposed:

$$\dot{D} = c\dot{\epsilon}^{p}_{eq} + (a_1 + a_2 D)(-Y)\dot{\epsilon}^{p}_{eq}. \tag{12}$$

Here, the first term, which is independent of $-Y$, represents the damage growth due to void nucleation, while the next two terms represent the evolution of damage due to void growth. The above expression states that void nucleation depends linearly on the equivalent plastic strain rate ($\dot{\epsilon}^{p}_{eq}$), which is in agreement with experimental results [7] and also consistent with Gurland's [11] model. Lemaitre [6], and Tai and Yang [12] did not consider the void nucleation term in their damage evolution law. Further, in Lemaitre's [6] work, the linear term in D is missing, while in the work of Tai and Yang [12], the term corresponding to a_1 is not considered.

In order to express $(-Y)$ in terms of the equivalent plastic strain (ϵ^{p}_{eq}), the relationship describing strain-hardening characteristics of the material is required. Here, it is assumed that the relationship is given by the following power law:

$$\sigma^{*}_{eq} = K(\epsilon^{p}_{eq})^{n} \tag{13}$$

where K and n are the material hardening parameters. Using this expression for σ^{*}_{eq} and the expression (3) for $(-Y)$, the damage evolution law [eq. (12)] can now be written as

$$\dot{D} = c\dot{\epsilon}^{p}_{eq} + (a_1 + a_2 D)\frac{K^2}{2E}(\epsilon^{p}_{eq})^{2n} f(\sigma^{*}_{m}/\sigma^{*}_{eq})\dot{\epsilon}^{p}_{eq}. \tag{14}$$

The constants c, a_1 and a_2 are determined by fitting the above equation through the experimental results of Le Roy *et al.* [7]. This is done in Section 3.

2.2. *The elasto-plastic matrix*

The incremental stress–strain relation is expressed as

$$\mathbf{d}\sigma = [C^{EP}]\mathbf{d}\epsilon \tag{15}$$

where $\mathbf{d}\sigma$ and $\mathbf{d}\epsilon$ are incremental stress and strain written in vector form. The $[C^{EP}]$ matrix is obtained from the plastic potential F_1 [eq. (10)] with the help of a flow rule following a standard procedure [13]. The expression for $[C^{EP}]$ is

$$[C^{EP}] = \left[[C] - \frac{[C]\mathbf{a}\mathbf{a}^{T}[C]^{T}}{H + \mathbf{a}^{T}[C]\mathbf{a}}\right](1 - D) \tag{16}$$

where $[C]$ is the elastic constitutive matrix. Further, flow vector

$$\mathbf{a}^{T} = \left[\frac{\partial F_1}{\partial \sigma^{*}_{xx}}, \frac{\partial F_1}{\partial \sigma^{*}_{yy}}, \ldots\right] \tag{17}$$

and the hardening parameter

$$H = \frac{\mathrm{d}\sigma^{*}_{eq}}{\mathrm{d}\epsilon^{p}_{eq}} \tag{18}$$

are obtained by differentiating eqs (10) and (13), respectively. In deriving $[C^{EP}]$ matrix, it is assumed that D does not change within the increment. D is updated only at the end of the increment.

2.3. *Crack initiation criterion*

Experimental studies on microstructural features of ductile fracture indicate that the ductile fracture process is essentially a localised plastic instability occurring simultaneously in the intervoid

matrix between a very large number of coalescing micro voids [8–10]. According to these references, the sufficient condition for plastic stability of the intervoid matrix at a point is given by

$$\sigma_1 - \sigma_n \bar{A}_n = 0 \tag{19}$$

where σ_1 is the current maximum principal stress of the macroscopically homogeneous state of stress at the point, $\bar{A}_n$ is the current effective area void fraction of the intervoid matrix at the point and σ_n is the critical stress required to initiate localised plastic flow or internal necking. The stress σ_n is called the plastic constraint stress.

Since there are about 10^5 micro voids in an area of approximately 0.25 mm^2 of ductile fracture surface [10], one can describe the fracture process by using a simple unit cell model in which the unit cell represents the statistical average of the micro void size and intervoid spacing at the point under consideration. The problem of finding an analytical expression for the plastic constraint stress σ_n in a unit cell with an ellipsoidal void seems to be intractable. Thomason [10] considered a geometrically equivalent square-prismatic void with the same principal dimensions as the ellipsoidal void and used the upper bound method to obtain the following expression for the plastic constraint stress:

$$\sigma_n = \left\{ \frac{0.1}{(a/d)^2} + \frac{1.2}{[b/(b+d)]^{1/2}} \right\} \sigma_{eq}^* \tag{20}$$

where a and b are the void dimensions, and d is the intervoid spacing (Fig. 1). This expression has been obtained by modifying the original expression of Thomason (which is for a perfectly plastic material) to incorporate the hardening of the material. Here, σ_{eq}^* is the current value of the yield stress of the intervoid material.

Elimination of σ_n from eqs (19) and (20) leads to the following expression for the micro crack initiation criterion:

$$\sigma_1 - \left\{ \frac{0.1}{(a/d)^2} + \frac{1.2}{[b/(b+d)]^{1/2}} \right\} \bar{A}_n \sigma_{eq}^* = 0. \tag{21}$$

Therefore, whenever the combination of the stress, and the void size and spacing at a point satisfies the above equation, micro crack initiation will take place at that point. Since the actual σ_n will be less than its upper bound estimate [eq. (20)], the above criterion will overestimate the critical combination of the stress, and the void size and spacing at micro crack initiation.

In the present work, a micro crack initiation criterion is needed in terms of a combination of stress and strain, and not as a combination of stress, and void size and spacing. Therefore, the

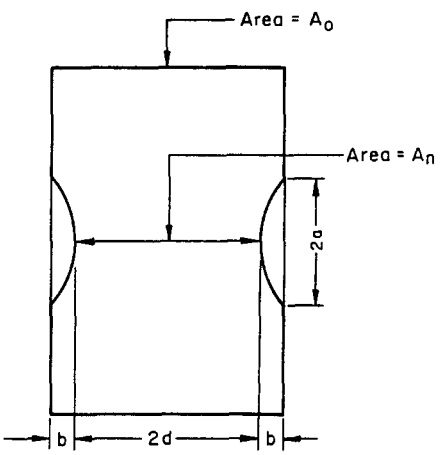

Fig. 1. Unit cell.

void dimensions a and b, the intervoid spacing d and the effective area ratio $\bar{A}_n$ should be expressed in terms of the strain at the point. Thomason suggested the Rice formula [2] to express a, b and d in terms of the strain. However, only a small strain is considered by Rice [2] in arriving at this formula. Therefore, it is not suitable for the case of large deformation.

Several research workers have suggested that, at micro crack initiation, the a/d ratio should lie between 0.8 and 1.2 depending on the triaxiality at the point. In the experimental results of Le Roy *et al.* [7], a/d is observed to be close to 1.0. Therefore, in this study, it is taken as 1.0. Thus,

$$a/d = 1.0. \tag{22}$$

To relate the void dimension b and the intervoid spacing d to the strain at the point, we assume that the equivalent strain

$$\epsilon_{eq} = \int_0^t \dot{\epsilon}_{eq}\, dt, \quad \dot{\epsilon}_{eq} = (\tfrac{2}{3}\dot{\epsilon}_{ij}\dot{\epsilon}_{ij})^{1/2} \tag{23}$$

at the point is more or less equal to the axial strain of the unit cell. Then, from Fig. 1 we get

$$\bar{A}_n = A_n/A_0 = \exp(-\epsilon_{eq}) \tag{24}$$

$$d/(b + d) = \exp(-\epsilon_{eq}/2). \tag{25}$$

The last equation implies

$$b/(b + d) = 1 - \exp(-\epsilon_{eq}/2). \tag{26}$$

Substituting eqs (22), (24) and (26) into eq. (21) we get

$$\sigma_1 - \left\{0.1 + \frac{1.2}{[1 - \exp(-\epsilon_{eq}/2)]^{1/2}}\right\} \exp(-\epsilon_{eq})\sigma_{eq}^{*} = 0. \tag{27}$$

This is the micro crack initiation criterion used in this study. It states that whenever a combination of stress and strain at a point satisfies the above equation, micro crack initiation takes place at that point.

2.4. *Finite element formulation*

The constitutive equation derived in Section 2.1 is used in the elasto-plastic finite element analysis. The scheme used is an updated Lagrangian Jaumann stress rate formulation, as it can properly model the large rotation and finite strain which are dominant ahead of the crack tip for ductile materials.

For an updated Lagrangian formulation, the virtual work expression at time $t + \Delta t$ is expressed in terms of the configuration at time t as

$$\int_{v^t} {}_tS_{ij}^{t+\Delta t}\delta({}_t\epsilon_{ij}^{t+\Delta t})\, dv^t = R^{t+\Delta t}. \tag{28}$$

The right superscript indicates the current configuration and the left subscript indicates the reference configuration. The tensor S_{ij} stands for the 2nd Piola Kirchoff stress tensor and ϵ_{ij} is the Green–Lagrange strain tensor which is work conjugate to S_{ij}. R on the right hand side stands for the virtual work done by surface tractions. Following Bathe *et al.* [14], eq. (28) is simplified as

$$\int_{v^t} {}_tC_{ijkl}^{EP}\, {}_t\Delta e_{kl}\delta({}_t\Delta e_{ij})\, dv^t + \int_{v^t} \sigma_{ij}^t\delta({}_t\Delta\eta_{ij})\, dv^t = R^{t+\Delta t} - \int_{v^t} \sigma_{ij}^t\delta({}_t\Delta e_{ij})\, dv^t \tag{29}$$

Table 1. Material-AISI 1090 steel; chemical composition (% wt)

C	Mn	P	S	Si	Fe
0.92	0.72	0.009	0.022	0.20	Balance

Table 2. Material-AISI 1090 steel; mechanical properties

ν	E	σ_0	σ_{uts}	ϵ_f	K	n
0.3	210 GPa	464 MPa	619 MPa	0.63	1115 MPa	0.19

where C^{EP}_{ijkl} is the tensor form of the $[C^{EP}]$ matrix [eq. (16)], σ_{ij} represents Cauchy stress tensor, and the linear and non-linear parts of the incremental strain tensor are given by

$$ {}_t\Delta e_{ij} = \tfrac{1}{2}({}_t\Delta u_{i,j} + {}_t\Delta u_{j,i}) \tag{30} $$

$$ {}_t\Delta \eta_{i,j} = \tfrac{1}{2}\, {}_t\Delta u_{k,i}\, {}_t\Delta u_{k,j}. \tag{31} $$

Note that ${}_t\Delta e_{ij}$ is the tensor form of the incremental strain $\mathbf{d}\epsilon$ appearing in eq. (15). Further, for large rotation, the stress increment $\mathbf{d}\sigma$ appearing in eq. (15) must be related to Jaumann stress rate. Thus, in terms of Jaumann stress rate, the incremental stress strain relation [eq. (15)] becomes

$$ \overset{\nabla}{\sigma}{}^t_{ij}\, \mathrm{d}t = {}_tC^{EP}_{ijkl}\, {}_t\Delta e_{kl}. \tag{32} $$

Once ${}_t\Delta e_{ij}$ is calculated by solving eq. (29), the Jaumann stress rate is determined from eq. (32) and the Cauchy stress at time $t + \Delta t$ is obtained from

$$ \sigma^{t+\Delta t}_{ij} = \sigma^t_{ij} + \overset{\nabla}{\sigma}{}^t_{ij}\, \mathrm{d}t + \sigma^t_{ip} \cap^t_{pj} \mathrm{d}t + \sigma^t_{jp} \cap^t_{pi} \mathrm{d}t, \tag{33} $$

where $\cap^t_{ij}$ is the spin tensor defined by

$$ \cap^t_{ij}\, \mathrm{d}t = \tfrac{1}{2}({}_t\Delta u_{j,i} - {}_t\Delta u_{i,j}). \tag{34} $$

At every time step the Cauchy stress and configuration are updated, and the iteration process is continued till the required load level is reached.

3. NUMERICAL RESULTS AND DISCUSSION

The FEM formulation developed in Section 2.4 has been implemented in an iterative fashion. That is, eq. (29) is solved for equilibrium till the unbalanced work in any iteration cycle is zero. The arc length method with Newton Raphson scheme is used for displacement controlled problem.

In each increment, Cauchy stress components are calculated from eq. (33) and hence, equivalent stress (σ_{eq}), mean stress (σ_m) and triaxiality (σ_m/σ_{eq}) are obtained. From incremental strain components (${}_t\Delta e_{ij}$), incremental equivalent strain ($\dot{\epsilon}_{eq}\, \mathrm{d}t$) and hence, incremental equivalent plastic strain ($\dot{\epsilon}^p_{eq}\, \mathrm{d}t$) is obtained which is added in subsequent increments to get the total equivalent plastic strain (ϵ^p_{eq}). Damage increment is obtained from eq. (14) which is added to the previous value to get the total damage. Elastic unloading equations are used when the current equivalent stress is less than that of the previous step. During unloading, calculations regarding equivalent plastic strain and damage are bypassed. For reloading, calculations for equivalent plastic strain and damage are restarted again from the point of unloading. Load is calculated from the nodal reactions at a particular cross-section. For a cylindrical specimen, true stress is calculated from the load (P) divided by area A of the minimum cross-section at the necked region. The logarithmic strain is calculated from the change in diameter in the necked portion using the formula $\epsilon = 2 \ln(d_0/d_c)$, where d_0 and d_c are the initial and current diameters, respectively. The programme is terminated when the crack initiation condition [eq. (27)] is satisfied. The values of quantities like damage, equivalent plastic strain, etc. calculated at this point are termed as their critical values.

The material used in this study is AISI-1090 spheroidised steel whose void growth curve is given in ref. [7]. The chemical composition and mechanical properties of the material are given in Tables 1 and 2, respectively.

The coefficients a_1, a_2 and c of the damage growth law are obtained from eq. (14) by rearranging as a relation between $dD/d\epsilon^p_{eq}$ and ϵ^p_{eq} and also using Bridgman's [15] formula to express triaxiality as a function of strain. Then, from the experimental results of Le Roy *et al.* [7], the slopes $dD/d\epsilon^p_{eq}$ are calculated at different strain levels. Finally, the coefficients a_1, a_2 and c are obtained by the method of least square curve fitting:

$$a_1 = 9.8 \times 10^{-04}\ \text{MPa}^{-1},\ a_2 = 1.86\ \text{MPa}^{-1},\ c = 1.84 \times 10^{-02}.$$

Five specimens with different geometry and loading conditions are studied. The geometries of the specimens are shown in Fig. 2. For all the cases except for the cracked plate, a total of 105 eight-noded isoparametric elements is used. For the cracked plate, the number of eight-noded isoparametric elements is 182 with crack-tip element size of (0.2 × 0.2 mm) for an effective crack length of 5.0 mm. The undeformed and deformed mesh patterns for cylindrical piece are shown in Fig. 3. It is worth noting here that a small imperfection of the order of 0.01 mm in diameter at the centre of the undeformed cylinder is introduced in order to simulate necking.

To check the accuracy of the results obtained from computer simulation, the true stress–logarithmic strain curve from computer simulation is compared with that obtained by Le Roy *et al.* [7] in an experiment with AISI-1090 steel (Fig. 4). The difference in stress levels is 8.0% at a strain level of 55.0% This shows that the damage growth law [eq. (14)] matches the material behaviour even after the ultimate point.

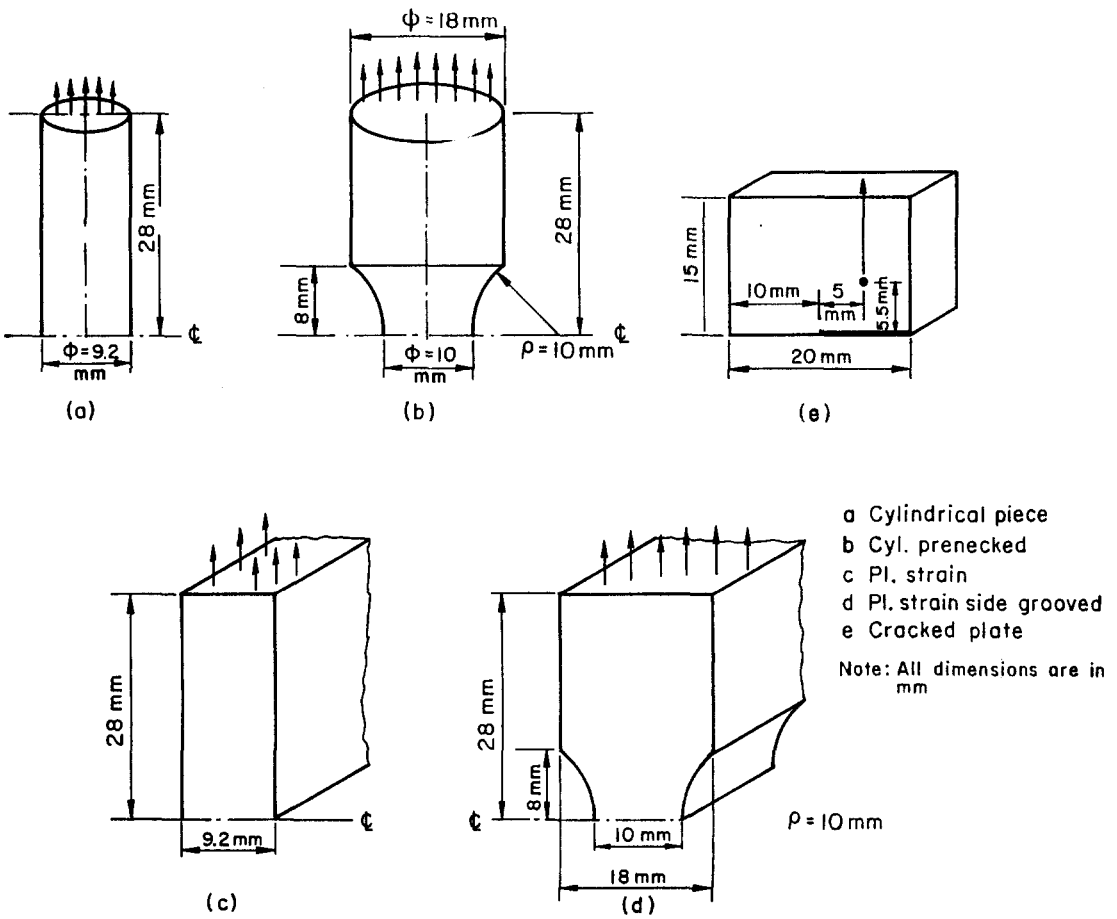

Fig. 2. Specimen geometry.

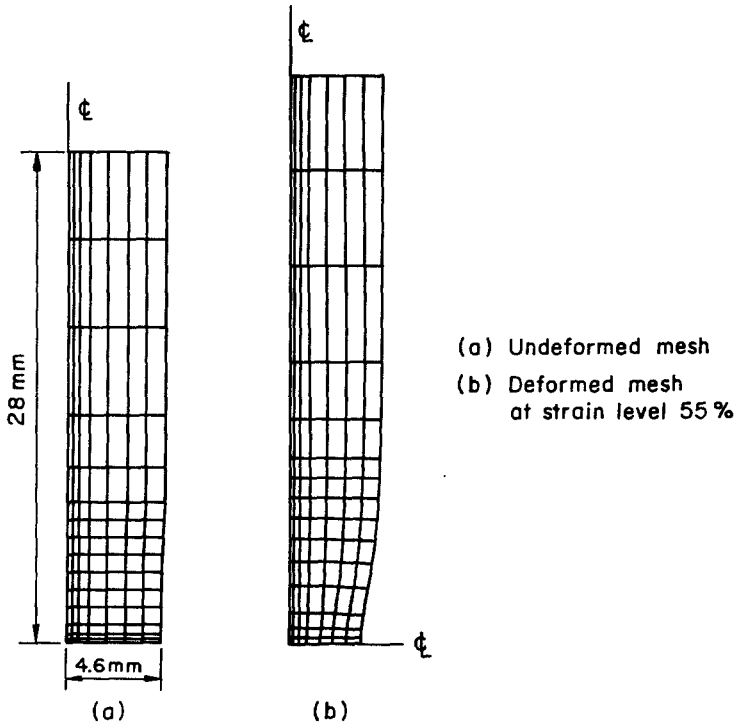

Fig. 3. Deformed and undeformed mesh patterns for cylindrical specimen.

Figure 5 shows the damage growth with equivalent plastic strain for the five cases. As expected, the damage grows with plastic strain. The critical values of damage (D_c) and strain $(\epsilon^p_{eq})_c$ are obtained when eq. (27) is satisfied. For all the cases except for the cracked plate, the maximum damage occurs at the centre. For the cracked plate, it occurs at the crack tip. The values of critical strain and critical damage for cylindrical test piece are, respectively, 60.6% and 5.62%. The reported value of fracture strain and the calculated value of critical area void fraction for cylindrical test piece in ref. [7] are, respectively, 63% and 5.3%. Since the value of critical strain is in good agreement with the experimental value, it shows that Thomason's model is a good representation of micro crack initiation.

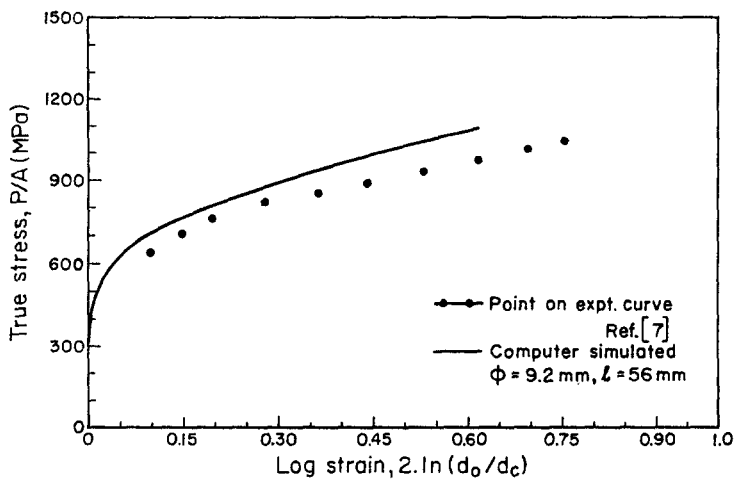

Fig. 4. Comparison of computer simulated true stress–logarithmic strain curve with experimental results for cylindrical specimen.

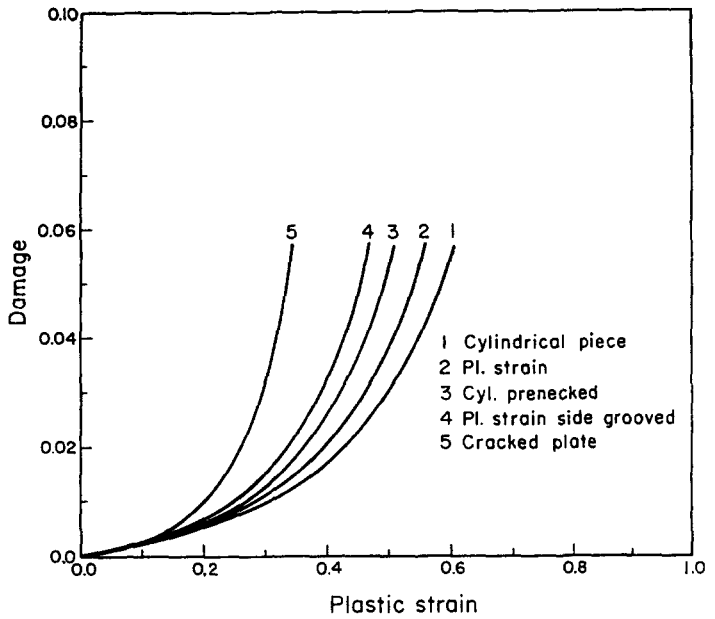

Fig. 5. Damage growth curves for fine specimens.

Figure 6 shows the variation of critical damage (D_c) with critical triaxiality $(\sigma_m/\sigma_{eq})_c$. It can be seen that although there is a wide variation in the values of critical triaxiality, the values of critical damage remain within a narrow band. From Figs 5 and 6, it is observed that for a wide variation of critical values of strain and triaxiality for different geometries, the critical value of damage remains almost the same. Hence, D_c can be regarded as a material property.

Figure 7 shows the variation of triaxiality with equivalent plastic strain for all the five cases. The locus of failure points is called the failure curve. The failure curve has a qualitative similarity with that of Hancock and Brown [16], but the quantitative comparison is not possible since they have used a different steel. This curve shows that failure can not be predicted either by critical strain alone or by critical triaxiality alone. Since one has to take into account both, it is better to predict

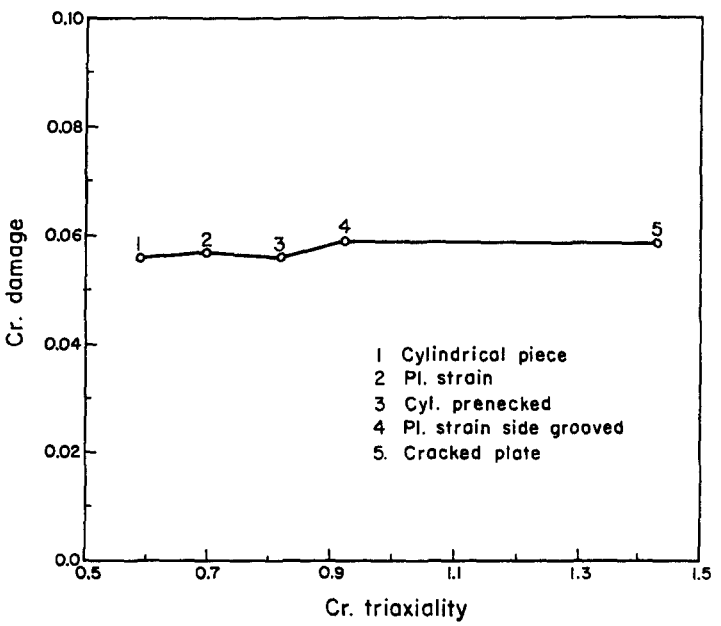

Fig. 6. Variation of critical damage with critical triaxiality.

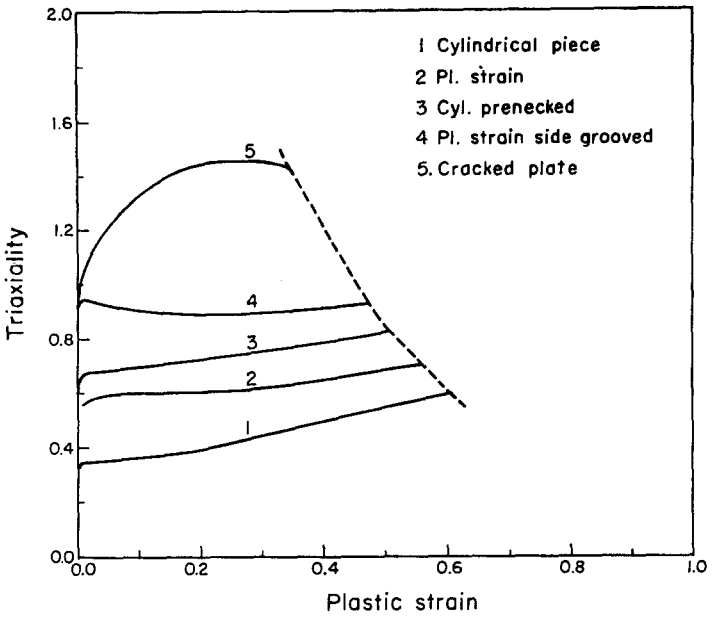

Fig. 7. Failure curve.

it by critical damage which incorporates both the strain and triaxiality. It is observed that critical strain increases with decreasing triaxiality. Finally, Fig. 7 shows that, besides strain, triaxiality also plays an important role in void growth and crack initiation.

4. CONCLUSIONS

The following conclusions can be drawn from the results of this study.

The damage growth law [eq. (14)] is proposed for void nucleation and growth for AISI-1090 spheroidised steel.

Thomason's micro model with a modification [eq. (27)] is proposed for crack initiation in incremental plasticity analysis.

From the study it is observed that the critical value of damage variable (D_c) can be considered as a material property for prediction of crack initiation in ductile materials.

The role of triaxiality in void growth and ductile fracture is well established from this study.

REFERENCES

[1] F. A. McClintock, A criteria for ductile fracture by growth of holes. *Trans. ASME, J. appl. Mech.* **35,** 363–371 (1968).
[2] J. R. Rice and D. M. Tracey, On the ductile enlargement of voids in triaxial stress fields. *J. Mech. Phys. Solids* **17,** 201–217 (1969).
[3] C. A. Berg, Plastic dilation and void interaction, in *Inelastic Behaviour of Solids* (Edited by Kanninen *et al.*), pp. 171–209. McGraw-Hill (1969).
[4] A. L. Gurson, Continuum theory of void nucleation and growth: Part I—Yield criteria and flow rules for porous ductile media. *Trans. ASME, J. Engng Mat. Tech.* **99,** 2–15 (1977).
[5] D. Know and R. J. Asaro, A study of void nucleation, growth and coalescence in spheroidised 1518 steel. *Metall. Trans. A* **21A,** 117–134 (1990).
[6] J. Lemaitre, A continuous damage mechanics model for ductile fracture. *Trans. ASME, J. Engng Mat. Tech.* **107,** 83–89 (1985).
[7] G. Le Roy, J. D. Embury, G. Edward and M. F. Ashby, A model of ductile fracture based on the nucleation and growth of voids. *Acta Metall.* **29,** 1509–1522 (1981).
[8] P. F. Thomason, Three dimensional models for the plastic limit loads at incipient failure of the intervoid matrix in ductile porous solids. *Acta Metall.* **33,** 1079–1085 (1985).
[9] P. F. Thomason, A three dimensional model for ductile fracture by the growth and coalescence of microvoids. *Acta Metall.* **33,** 1087–1095 (1985).
[10] P. F. Thomason, *Ductile Fracture of Metals*, Sections 1.6, 3.3, 3.4 and 5.3. Pergamon Press, Oxford (1990).
[11] J. Gurland, Observation on the fracture of cementite particles in a spheroidised 1.05%c steel deformed at room temperature. *Acta Metall.* **20,** 735–741 (1972).

[12] W. H. Tai and B. X. Yang, A new microvoid-damage model for ductile fracture. *Engng Fracture Mech.* **25,** 377–384 (1986).
[13] D. R. J. Owen and E. Hinton, *Finite Element in Plasticity: Theory and Practice*. Pineridge Press, Swansea, U.K. (1990).
[14] K. J. Bathe, E. Ramm and E. L. Wilson, Finite element formulations for large deformation dynamic analysis. *Int. J. Num. Meth. Engng* **9,** 353–386 (1975).
[15] P. W. Bridgman, *Studies in Large Plastic Flow and Fracture*. McGraw Hill, New York (1952).
[16] J. W. Hancock and D. K. Brown, On the role of strain and stress in ductile fracture. *J. Mech. Phys. Solids* **31,** 1–24 (1983).

(*Received* 7 *November* 1994)